

Calculated and experimental low-loss electron energy loss spectra of dislocations in diamond and GaN

This article has been downloaded from IOPscience. Please scroll down to see the full text article.

2002 J. Phys.: Condens. Matter 14 12793

(<http://iopscience.iop.org/0953-8984/14/48/318>)

View [the table of contents for this issue](#), or go to the [journal homepage](#) for more

Download details:

IP Address: 171.66.16.97

The article was downloaded on 18/05/2010 at 19:13

Please note that [terms and conditions apply](#).

Calculated and experimental low-loss electron energy loss spectra of dislocations in diamond and GaN

R Jones¹, C J Fall¹, A Gutiérrez-Sosa², U Bangert², M I Heggie³,
A T Blumenau⁴, T Frauenheim⁴ and P R Briddon⁵

¹ School of Physics, University of Exeter, Exeter EX4 4QL, UK

² Physics Department, UMIST, Manchester M60 1QD, UK

³ CPES, University of Sussex, Brighton BN1 9QJ, UK

⁴ Theoretische Physik, Universität Paderborn, D-33098 Paderborn, Germany

⁵ Department of Physics, University of Newcastle, Newcastle upon Tyne NE1 7RU, UK

E-mail: r.jones@exeter.uk

Received 1 October 2002

Published 22 November 2002

Online at stacks.iop.org/JPhysCM/14/12793

Abstract

First-principles calculations of electron energy loss (EEL) spectra for bulk GaN and diamond are compared with experimental spectra acquired with a scanning tunnelling electron microscope offering ultra-high-energy resolution in low-loss energy spectroscopy. The theoretical bulk low-loss EEL spectra, in the E_g to 10 eV range, are in good agreement with experimental data. Spatially resolved spectra from dislocated regions in both materials are distinct from bulk spectra. The main effects are, however, confined to energy losses lying above the band edge. The calculated spectra for low-energy dislocations in diamond are consistent with the experimental observations, but difficulties remain in understanding the spectra of threading dislocations in GaN.

1. Introduction

The atomic and electronic structure of dislocations in semiconductors is a topic of considerable current interest. In GaN, the electrical and structural properties of screw dislocations have been observed to depend sensitively on the growth conditions [1]. Full-core structures are expected to lead to gap states, which if filled would lead to dislocation line charging. Scanning capacitance spectroscopy results have suggested that GaN threading dislocations are negatively charged [2], as have electron holography measurements [3]. A recent ballistic electron emission microscopy study has, however, concluded that threading dislocations do not have a fixed negative charge, and are, if anything, positively charged at the surface [4].

Initial theoretical investigations of GaN open-core screw and edge dislocations suggested that dislocation core reconstructions lead to a lack of deep gap states [5]. Subsequent calculations, however, have predicted deep levels associated with GaN edge dislocations, leading in particular to charge accumulation at dislocations [6, 7]. Furthermore, a recent

theoretical study of GaN edge dislocations has shown evidence for empty gap states associated with full-core GaN edge dislocations in the top half of the gap [8].

The growth of polycrystalline chemically vapour deposited (CVD) diamond generates high densities of dislocations (up to 10^{12} cm^{-2}), which originate in the substrate–interface region and can propagate throughout the thin film [9]. Such extended defects have been correlated with band-A cathodoluminescence observed at 2.8–2.9 eV in undoped CVD diamond [10, 11] and natural type-II diamond [12, 13]. It has recently been suggested that colour changes produced in natural brown diamonds by high-pressure high-temperature annealing are linked to changes in dislocation structure [14].

Low-loss electron energy loss (EEL) spectroscopy, in the 0–20 eV range, where the energy loss is induced by exciting electrons from occupied to empty bands, is a technique that can be performed in a scanning tunnelling electron microscope (STEM) that leads directly to detailed information about gap states. Cross-sectional low-loss EEL experiments in GaN have shown differences in the onset of the EEL spectrum on and off threading dislocations [15]. Recent, low-loss EEL spectroscopy investigations in brown diamonds have also been interpreted in terms of dislocation-related gap states [16].

In this paper, we review first-principles simulations of the low-loss EEL spectrum arising from dislocation cores in GaN and diamond and compare the results with experimental spectra. Further details of the method and experimental conditions are given in recent papers [17–20].

2. Theoretical and experimental methods

2.1. Theoretical method

We carry out *ab initio* local density functional (LDF) calculations of wurtzite GaN and cubic diamond using a real-space Cartesian Gaussian basis set within the AIMPRO code [21].

For GaN, we consider two complementary approaches when describing dislocations:

- (a) a pair of edge dislocations with opposite Burgers vectors is inserted in a 144-atom supercell, or
- (b) a single edge dislocation is located centrally in a 120-atom cylinder whose surface dangling bonds are saturated by fractionally charged hydrogen-like atoms.

Both techniques describe [0001] dislocations of infinite length. The periodicity of the structures along [0001] is fixed at the bulk value. In approach (a), the dislocations are arranged in a quadrupole lattice to minimize strain effects [22]. In approach (b), we include at least 20 au of vacuum around the surface hydrogen atoms. In the case of diamond, we used the hydrogenated clusters inside supercells with 60- to 160-atom supercells. Initial relaxations of the dislocation cores are performed using the self-consistent charge density functional tight-binding method (scc-DFTB) [23, 24] with clusters of up to 500 atoms. The atoms are then further relaxed with AIMPRO to their equilibrium positions, using two reduced MP k -points along the dislocation line.

Low-loss EEL spectra result from electronic transitions between filled valence bands (VB) and empty conduction bands (CB). Transitions involving gap states contribute to the EEL spectra and allow defects to be probed. The signal obtained experimentally is representative of $-\text{Im } \varepsilon(E)^{-1}$, where $\varepsilon = \varepsilon_1 + i\varepsilon_2$ is the dielectric function and E is the energy loss [25]. We calculate the diagonal elements of the imaginary part of the dielectric function in the dipole approximation for an applied electron beam oriented along a direction either parallel or perpendicular to the dislocation line [26, 27]. The LDF bandgap is adjusted to the experimental value by shifting the CB. Gap states are shifted proportionally to their distance from the VB. The real

part of the dielectric function is obtained through a Kramers–Kronig (KK) transformation. The BZ integrations are performed in bulk material using 1024 MP k -points and a similar k -point density in the supercells. In view of the number of atoms in our supercells, we are therefore modelling an EEL spectrum acquired with an electron beam probe diameter of 10–15 Å, centred exactly at the dislocation core. This size is similar to current experimental values [15].

Although the above formalism is expected to give good results for low-loss spectra for direct-bandgap materials, for example GaN, there are additional issues for materials with an indirect bandgap [28]. For example, in 3C-SiC, where the direct and indirect bandgaps are calculated to be 6.46 and 1.35 eV, the above formalism gives the calculated EEL onset at the former while the observed onset is at the indirect gap at 2.3 eV. The effect of indirect transitions is expected to be most important for the bulk as the dislocation-related dispersion is relatively flat and hence the direct and indirect bandgaps arising from the dislocation-related bands are similar. For diamond, the indirect gap is only 0.5 eV lower than the direct one and hence these complications are not expected to be significant.

2.2. Experimental details

Experimental low-loss EEL spectra were found using a VG601 cold field emission STEM, operating at 100 kV, with a probe size of around 10 Å. For losses greater than about 2 eV, the energy resolution can be increased by selecting a higher energy dispersion for the spectrometer. This was selected to be 0.01 eV/channel in the present investigation. The number of spectra, the acquisition time per spectrum and the gun extraction voltage were chosen so that they gave a FWHM of the zero-loss peak of 0.34–0.36 eV. This then leads to an ultra-high-energy resolution of 0.18 eV. In the case of GaN, spectra were taken at points along, and off, threading dislocations with the electron beam perpendicular to the dislocation line. In contrast to studies where the beam was directed along the c -axis, this procedure led to a low-loss spectrum exhibiting differences between bulk and dislocated regions.

The GaN sample used here consisted of two GaN layers grown on sapphire, each of width ~ 1 μm . The bottom layer was n-type while the top layer had been doped with Mg and was either p-type or semi-insulating. The diamond sample was prepared by ion thinning a 0.84 μm thick membrane of boron-doped polycrystalline CVD diamond grown on a 3-inch diameter {100} oriented silicon wafer at 800 °C. The boron concentration was 2×10^{21} cm^{-3} .

The diamond contained such a high density of grain boundary dislocations that it was difficult to find defect-free material. Many stacking faults were present, and although similar results were found for the many dislocations, attention was focused on one partial dislocation thought to be a 30° lying along $\langle 110 \rangle$.

It should be emphasized that the relative intensities of the experimental spectra are expected to be different from those of the simulated spectra: the ratio of the bulk and dislocation volume in the experiment may vary between sampling points as the sample thickness varies; it is moreover generally larger than that used in the spectrum calculations. More details of the theoretical and experimental procedures as well as sample preparation are reported elsewhere [17–19].

3. Results and discussion

3.1. Dislocations in GaN

The calculated low-loss EEL spectra of bulk GaN and AlN are found to be in good agreement with corresponding experimental data [17]. This close correspondence gives us confidence that the calculations can simulate the EEL spectra of extended defects. The relaxed geometry and band structure of a neutral GaN threading edge dislocation is shown in figure 1, using the

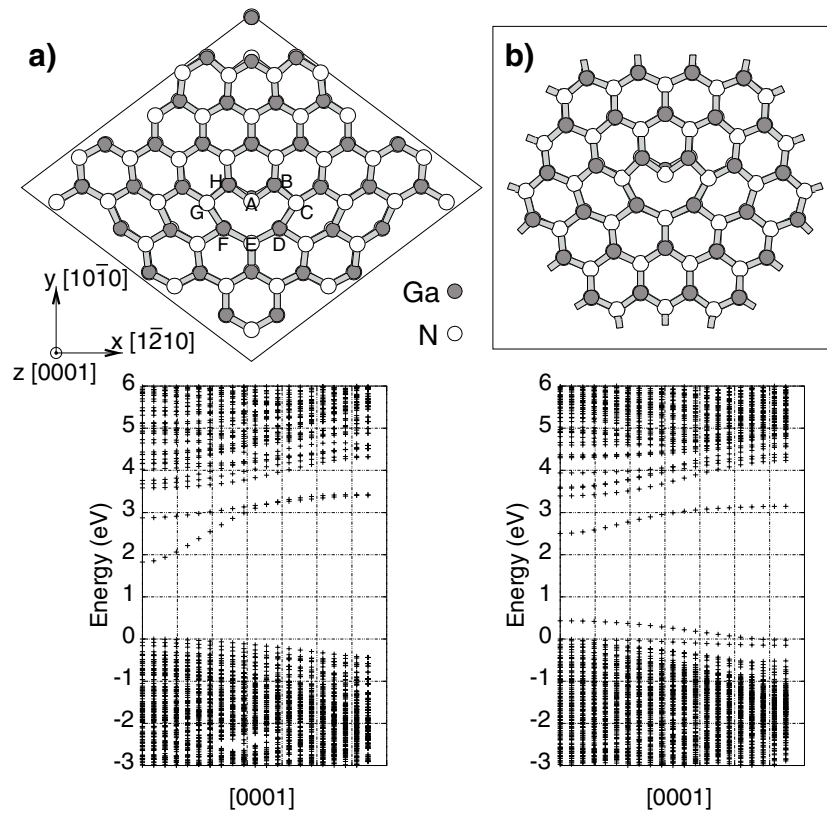


Figure 1. Upper panels: two complementary approaches for describing dislocations: (a) a GaN supercell containing two edge dislocations; (b) a GaN single edge dislocation surrounded by a vacuum, where the surface bonds are saturated by fractional hydrogen atoms (not shown). Both structures have been fully relaxed in the neutral charge state. The N atoms are shown in white and Ga atoms in grey. In the displayed band structure the one-dimensional BZ is shown from 0 to π/c where c is the lattice constant along [0001]. The core atomic columns are indexed with capital letters. Lower panels: corresponding band structures in the [0001] c -direction. The reference energy has been set at the top of the filled valence states. All levels in the top (bottom) half of the gap are empty (filled, respectively).

two supercell techniques described in section 2.1. In both approaches, empty states localized at the core of the dislocation are found in the upper half of the gap.

By comparing the band structures obtained in the two prescriptions for treating dislocations some differences can be seen. Although empty and filled bands are always in the same part of the gap, the strain induced by the dislocations in approach (a) is over-estimated with respect to an isolated dislocation in an otherwise perfect infinite crystal because of the computationally restricted supercell size. Conversely, in approach (b), because the supercell surface is free to relax entirely, the dislocation strain is underestimated, and creates a bending of the $(10\bar{1}0)$ atomic planes parallel to the Burgers vector. This distortion is responsible, for example, for creating an artificially raised filled level ~ 0.4 eV above the VB (see lower right panel of figure 1). Overall, these results conclusively show that neutral edge dislocations, expected to be present in p-type material, possess levels in the gap that lead to supplementary EEL absorption.

The effect of charging the dislocation was investigated by adding a pair of electrons per repeat distance c . The effect was to *lower* the dislocation-related states and introduce a new empty band similar to that found in an earlier study [6].

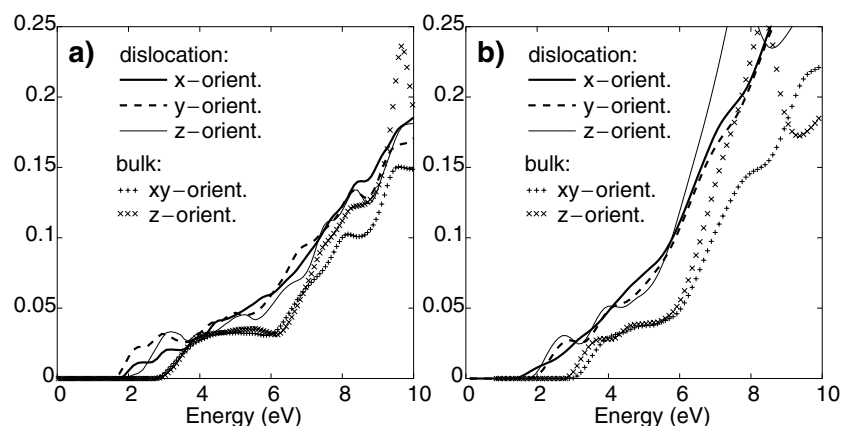


Figure 2. Comparison between the computed EEL spectra of a region containing a neutral GaN edge dislocation (curves) and bulk GaN (symbols). The results are shown for the two unit cells with dislocations shown in figure 1. In panel (b), the dislocation EEL spectrum is compared with a bulk spectrum determined in a similar bulk hybrid supercell. In panel (b), the spectra have been rescaled to bring the highest peaks of the EELS spectra (not shown) in agreement with those found in panel (a), thus accounting for the vacuum region of the supercell. Results are given for an electron beam oriented along x , y and z , using the coordinate system defined in figure 1.

The computed energy loss spectrum for the neutral edge dislocation is presented in figure 2 where it is compared with a bulk spectrum calculated in a similar way. In view of the gap states created by the edge dislocation, additional absorption in the EEL spectrum is found below the bulk band edge. An electron beam directed parallel to the basal plane is seen to lead to absorption at lower energies than with the beam oriented along the c -axis. Some supplementary absorption is also observed in the 5–7 eV range and eliminates the plateau seen for bulk in this region. Comparing the results obtained using the supercell and hybrid approaches gives some idea of the accuracy of our modelled spectra. We note that the hybrid approach leads to a spectrum which rises more strongly above 6 eV, although the changes in absorption compared with bulk are similar to those found in figure 2(a). These results make visible the importance of boundary conditions when calculating the electronic properties of dislocations. The simulated EEL spectrum for a threading screw dislocation is similar to the edge except that both occupied and empty bands are found in the gap [17].

Figure 3 shows the experimental low-loss spectra for a threading dislocation in the GaN sample lying in both n-type and p-type regions. Spectra (a)–(c) arise from a threading mixed dislocation in n- and p-type material acquired when the electron beam was perpendicular to the dislocation line. Spectrum (d) is for the bulk material. The bottom four spectra are difference spectra like (a)–(d) with the last being the difference spectra recorded from two bulk regions. The most obvious difference is the elimination of the plateau region seen for bulk from 4 to 8 eV, and this agrees with the calculated spectrum shown in figure 2. The difference spectra, in the 2–3.5 eV range, suggest the presence of gap states close to E_c but there is no dramatic difference between n- and p-type regions as expected by the theory.

3.2. Dislocations in diamond

In diamond, dislocations lie predominantly on $\{111\}$ planes. Glide and shuffle dislocations differ from each other in that the removed half-plane of atoms terminates after a long or a short interplane separation in the $[111]$ direction respectively and 60° glide dislocations are

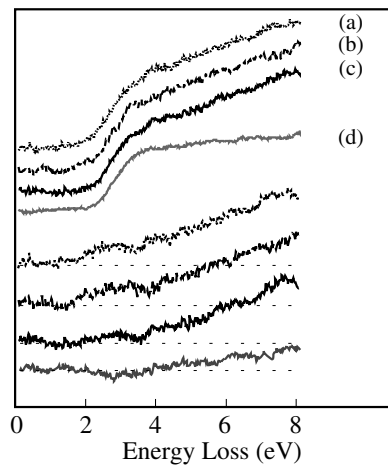


Figure 3. From top to bottom, experimental EEL spectra for mixed threading dislocation in (a) an n-type region of GaN; (b) and (c) are in p-type regions; (d) is the spectrum of the bulk. Spectra are normalized at 9 eV. Difference spectra (a)–(d), (b)–(d), (c)–(d), (d) are shown in lower panel. The bottom curve is the difference spectrum from two regions of bulk material. Note the elimination in (a)–(c) of the plateau region seen in the bulk spectrum (d) from 4 to 8 eV and the presence of gap states near E_c .

known to dissociate into 30° and 90° partial dislocations separated by an intrinsic stacking fault [29, 30]. Screw dislocations in diamond have also been observed to dissociate into partials [31]. We have recently reported the structure [24] and low-loss EEL spectrum for a number of dislocations in diamond [18] and here will only discuss the 30° double-period reconstructed partial dislocation. Figure 4 shows the calculated electronic band structure, low-loss and core EEL spectra. The calculations suggest that much larger dislocation effects are expected when the electron beam is oblique to the dislocation line. Indeed, the calculated spectra in the 6–10 eV region obtained for an electron beam incidence perpendicular to the dislocation line (full and dashed curves in figure 4, when compared with bulk, suggest additional loss in the 6–8 eV region. Consistent with this is the experimental spectrum shown as a dashed curve in figure 5, taken with the electron beam parallel to $\langle 111 \rangle$. This spectrum is due to a partial dislocation, presumably a dissociated screw, i.e. a 30° glide partially bounding a stacking fault. The dislocation line presumably lies along $\langle 110 \rangle$ and is oblique with respect to the beam direction. Unfortunately, the high density of dislocations prevented a TEM identification of the Burgers vector. No gap absorption is detected, showing that these dislocations appear electrically inactive. Incidentally, figures 4 and 5 show that the observed and calculated low-loss spectra of bulk diamond are in good agreement with each other.

4. Conclusions

In this paper we have computed from first principles the low-loss electron energy loss spectra of dislocations in GaN and diamond and compared the spectra with experimental studies which achieve ultra-high-energy resolution. In neither case was there any experimental evidence for deep mid-gap states although there are problems in resolving energy losses of 2 eV or less. Whereas this is in accordance with theoretical expectations for the low-energy dislocations in diamond, it is not the case for threading dislocations in GaN where empty gap states in the upper half of the gap should be present. In both diamond and GaN, the observed EEL spectrum

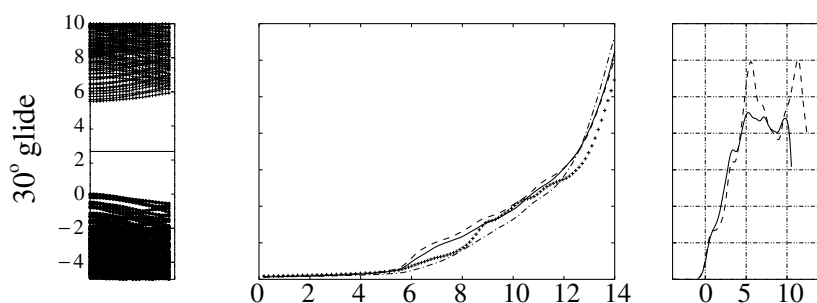


Figure 4. Band structure along the dislocation core in the [110] direction in the gap region, low-loss EEL spectrum, and predicted K-edge core EEL spectrum for 30° glide dislocation in diamond. In the displayed band structure the one-dimensional BZ is shown from 0 to $\pi/\sqrt{2}/a$ where a is the lattice constant. In the band structure, the filled and empty states of neutral dislocation are separated by a horizontal line. The low-loss EEL spectra are shown for incident beams oriented in the $[1\bar{1}2]$ (solid curve) and $[1\bar{1}1]$ (dashed curve) directions orthogonal to the dislocation axis, as well as along the [110] dislocation axis (dash-dot curve), and are compared with superimposed bulk spectra superimposed (crosses). For core EEL spectroscopy, dislocation spectra (solid curves) are compared with bulk spectra (dashed curves). The energy zero is set at the CB minimum in both cases. All energy scales are given in eV.

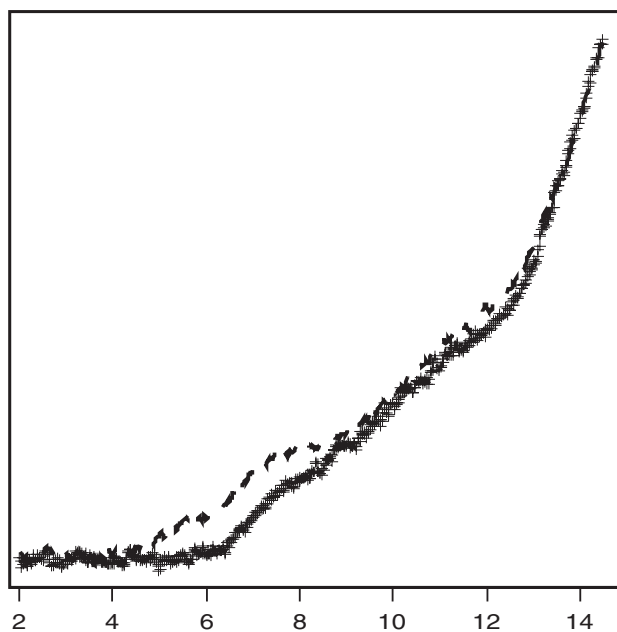


Figure 5. Experimental low-loss EEL spectra for bulk (crosses) and oblique partial dislocation in diamond (dashed curve) with the electron beam along $\langle 111 \rangle$. Energy scale in eV.

taken from regions containing dislocations is different from that of bulk. Hence, it is clear that the dislocations perturb the EEL spectrum eliminating the plateau in GaN and leading to additional loss in the 5–10 eV range in diamond. In the case of GaN there is some evidence for gap states close to E_c (see the difference spectra in figure 3) but no dramatic difference between p- and n-type regions as expected. It may be that the doping is ineffective or that impurities or

point defects affect the experimental spectra actually removing states from the energy gap in GaN. However, calculations incorporating hydrogen into the core in GaN did not find this to occur. On the other hand, point defects may be responsible for band-A cathodoluminescence in diamond. Nevertheless, these first combined experimental and theoretical studies have been productive and are likely to lead to further developments.

References

- [1] Hsu J W P, Manfra M J, Chu S N G, Chen C H, Pfeiffer L N and Molnar R J 2001 *Appl. Phys. Lett.* **78** 3980
- [2] Schaadt D M, Miller E J, Yu E T and Redwing J M 2001 *Appl. Phys. Lett.* **78** 88
- [3] Cherns D and Jiao C G 2001 *Phys. Rev. Lett.* **87** 205504
- [4] Im H-J, Ding Y, Pelz J P, Heying B and Speck J S 2001 *Phys. Rev. Lett.* **87** 106802
- [5] Elsner J, Jones R, Stich P K, Porezag V D, Elstner M, Frauenheim T, Öberg S and Briddon P R 1997 *Phys. Rev. Lett.* **79** 3672
- [6] Wright A F and Grossner U 1998 *Appl. Phys. Lett.* **73** 2751
- [7] Leung K, Wright A F and Stechel E B 1999 *Appl. Phys. Lett.* **74** 2495
- [8] Lee S M, Belkhir M A, Zhu X Y, Lee Y H, Hwang Y G and Frauenheim T 2000 *Phys. Rev. B* **61** 16033
- [9] Graebner J E, Reiss M E, Seibles L, Hartnett T M, Miller R P and Robinson C J 1994 *Phys. Rev. B* **50** 3702
- [10] Ruan J, Kobashi K and Choyke W J 1992 *Appl. Phys. Lett.* **60** 3138
- [11] Takeuchi D, Watanabe H, Yamanaka S, Okushi H, Sawada H, Ichinose H, Sekiguchi T and Kajimura K 2001 *Phys. Rev. B* **63** 245328
- [12] Kiflawi I and Lang A R 1974 *Phil. Mag.* **30** 219
- [13] Hanley P L, Kiflawi I and Lang A R 1977 *Phil. Trans. R. Soc. A* **284** 329
- [14] Collins A T, Kanda H and Kitawaki H 2000 *Diamond Relat. Mater.* **9** 113
- [15] Gutiérrez-Sosa A, Bangert U, Harvey A J, Flavell W R, Jacobs K, Moermann I and Rizzi A 2001 *Inst. Phys. Conf. Ser.* **169** 255
- [16] Kolodzie A T, Murfitt M and Bleloch A 2001 *Inst. Phys. Conf. Ser.* **168** 247
- [17] Fall C J, Jones R, Briddon P R, Blumenau A T, Frauenheim T and Heggie M I 2002 *Phys. Rev. B* **65** 245304
- [18] Fall C J, Blumenau A T, Jones R, Briddon P R, Frauenheim T, Gutiérrez-Sosa A, Bangert U, Mora A E, Steeds J W and Butler J E 2002 *Phys. Rev. B* **65** 205206
- [19] Gutiérrez-Sosa A, Bangert U, Harvey A J, Fall C J, Jones R, Briddon P R and Heggie M I 2002 *Phys. Rev. B* **66** 035302
- [20] Blumenau A T, Fall C J, Jones R, Heggie M I, Frauenheim T, Briddon P R and Öberg S 2002 *J. Phys.: Condens. Matter* **14**
- [21] Briddon P R and Jones R 2000 *Phys. Status Solidi b* **217** 131
- [22] Bigger J R K, McInnes D A, Sutton A P, Payne M C, Stich I, King-Smith R D, Bird D M and Clarke L J 1992 *Phys. Rev. Lett.* **69** 2224
- [23] Frauenheim T, Seifert G, Elstner M, Hajnal Z, Jungnickel G, Porezag D, Suhai S and Scholz R 2000 *Phys. Status Solidi b* **217** 41
- [24] Blumenau A T, Heggie M I, Fall C J, Jones R and Frauenheim T 2002 *Phys. Rev. B* **65** 205205
- [25] Nozières D and Pines D 1959 *Phys. Rev.* **113** 1254
- [26] Bassani G F and Pastori Parravicini G 1975 Electronic states and optical transitions in solids *Int. Series of Monographs in the Science of the Solid State* vol 8, ed R A Ballinger (Oxford: Pergamon)
- [27] Read A J and Needs R J 1991 *Phys. Rev. B* **44** 13071
- [28] Rafferty B and Brown L M 1998 *Phys. Rev. B* **58** 10326
- [29] Nunes R W, Bennetto J and Vanderbilt D 1998 *Phys. Rev. B* **58** 12563
- [30] Pirouz P, Cockayne D J H, Sumida N, Hirsch Sir P and Lang A R 1983 *Proc. R. Soc. A* **386** 241
- [31] Luyten W, Van Tendeloo G, Amelinckx S and Collins L J 1992 *Phil. Mag. A* **66** 899